CDDpress

www.nature.com/cdd

ARTICLE OPEN

Check for updates

Role of the cross-regulation between Wnt pathway activation and androgen receptor signaling in prostate cancer treatment resistance

Nicolas Anselmino[1,2✉], Pablo Sanchis[1,3,4,5], Juan Bizzotto[3,4,5], Estefania Labanca[1], Jiabin Dong[1], Peter D. A. Shepherd[1], Jun Yang[1], Elba S. Vazquez[3,4], Joaquin Mateo[2,6], Geraldine Gueron[3,4] and Christopher J. Logothetis[1]

Prostate cancer (PCa) is a biologically heterogeneous disease that frequently progresses to castration-resistant prostate cancer (CRPC), a challenging clinical stage. The underlying mechanisms driving CRPC progression and resistance to androgen receptor (AR) signaling inhibition (ARSI) remain incompletely understood. Emerging evidence implicates the canonical Wnt pathway as a key contributor to CRPC progression. This study elucidates the role of Wnt pathway activation in mediating resistance to ARSI and identifies a robust molecular signature for predicting treatment outcomes. By integrating genomic and transcriptomic data from PCa patients, patient-derived xenografts (PDXs), and experimental models harboring or not Wnt-activating mutations, we performed differential expression analysis, unsupervised clustering, survival, and viability analysis to assess Wnt/β-catenin pathway activation and its interaction with AR signaling. A specific Wnt transcriptional signature (*AXIN2*, *RNF43*, *ZNRF3*, *NKD1*) was found to reliably reflect pathway activation in advanced PCa. AR was found to suppress mutation-driven Wnt signaling, which was upregulated upon AR inhibition, contributing to treatment resistance. Targeting β-catenin interactions with co-activators p300/CBP using selective inhibitors (IQ-1 and ICG-001) effectively mitigated Wnt-driven ARSI resistance, restoring sensitivity to therapy in preclinical models. Thus, canonical Wnt pathway activation emerges as a critical mediator of resistance to ARSI in CRPC. The identified Wnt signature holds potential as a biomarker for predicting and monitoring therapeutic outcomes. Concurrent targeting of AR and Wnt signaling represents a promising strategy to overcome treatment resistance, particularly in patients with Wnt-activating mutations.

Cell Death & Differentiation; https://doi.org/10.1038/s41418-026-01732-7

INTRODUCTION

The biological heterogeneous nature of prostate cancer (PCa) accounts for the challenges in curing advanced disease [1, 2]. Despite recent advances in molecular classification and precision oncology, the progression to castration-resistant PCa (CRPC) is incompletely understood. Resistance mechanisms have been linked to androgen receptor (AR) pathway reactivation as well as other compensatory survival pathways, leading to treatment-refractory progression [1]. However, the gap in the identification of the drivers of CRPC progression is reflected in the significant number of patients who do not benefit from current therapeutic approaches. Several reports link the Wnt canonical pathway to progression in different cancers, including PCa [3–7]. Wnt plays pivotal roles in regulating key cellular processes, such as proliferation, differentiation, and survival [8, 9]. Genomic studies in metastatic PCa revealed that 10–20% of cases harbor mutations in Wnt-related genes, most notably *CTNNB1* (β-catenin) and *APC* [10, 11]. These mutations, known to drive aberrant activation of Wnt/β-catenin signaling, correlate with tumor progression, resistance to AR signaling inhibition (ARSI) -a standard treatment for advanced PCa- [3], and shorter progression-free and overall survival [4]. However, the full impact of Wnt signaling in PCa and its interaction with AR signaling is poorly understood. Cross-regulation between the Wnt/β-catenin and AR pathways has been proposed [12–14], but the nature of this interplay, especially in the context of AR inhibition, is still under investigation. The purpose of this study was to further assess the role of Wnt activation in CRPC and its implications on ARSI resistance.

Integrating genomic and transcriptomic data from PDXs, clinical samples, and experimental models, we identified a Wnt-specific signature reflecting canonical pathway activation in advanced PCa. The interplay between Wnt and AR signaling underscored a novel resistance mechanism to AR-targeted therapies. Additionally, β-catenin blockade restored responsiveness to ARSI,

[1]Department of Genitourinary Medical Oncology and the David H. Koch Center for Applied Research of Genitourinary Cancers, The University of Texas MD Anderson Cancer Center, Houston, TX, USA. [2]Prostate Cancer Research Group, Vall d'Hebron Institute of Oncology (VHIO), Vall d'Hebron University Hospital, Barcelona, Spain. [3]Laboratorio de Inflamación y Cáncer, Departamento de Química Biológica, Facultad de Ciencias Exactas y Naturales, Universidad de Buenos Aires, Buenos Aires, Argentina. [4]Instituto de Química Biológica de la Facultad de Ciencias Exactas y Naturales (IQUIBICEN), CONICET-Universidad de Buenos Aires, Buenos Aires, Argentina. [5]Instituto de Tecnología (INTEC), Universidad Argentina de la Empresa (UADE), Buenos Aires, Argentina. [6]Department of Medical Oncology, Vall d'Hebron University Hospital and Vall d'Hebron Institute of Oncology (VHIO), Barcelona, Spain. ✉email: nicolasanselmino@vhio.net; nicoanselmino@gmail.com

Received: 11 September 2025 Revised: 12 February 2026 Accepted: 17 March 2026
Published online: 14 April 2026

highlighting Wnt activation as both a clinically relevant biomarker and a targetable vulnerability in advanced PCa.

METHODS

Cell culture

PC3 (CRPC AR-), C42B (AR+, sensitive to AR inhibition), and LNCaP (androgen dependent, AR+) cells were purchased from the American Type Culture Collection (Manassas, VA, USA) and maintained in RPMI-1640 (Millipore-Sigma, Burlington, MA, USA) supplemented with 10% FBS (Millipore-Sigma).

Genetically modified cell lines

β-catenin variant sublines were developed from parental cell lines by stably transducing them with lentivirus carrying pLenti-C-mGFP-P2A-BSD vectors for the expression of β-catenin WT or mutant variants D32G or T41A, or with no insert (EV) as a control (OriGene, Rockville, MD). D32G and T41A mutations are among the widely described β-catenin activating mutations associated with pathogenicity that were present among the MDA PCa PDX cohort [10, 15–20]. Stably transduced cells were selected with blasticidin (8 μg/mL) (InvivoGen, San Diego, CA, USA).

Animals

Practices involving laboratory animals were conducted under the approval of the Institutional Animal Care and Use Committee of The University of Texas MD Anderson Cancer Center and conform to the Animal Welfare Committee (IACUC) and NIH Policy on Humane Care and Use of Laboratory Animals.

In vivo relapse

Six-to-eight-week-old male CB17-*SCID* mice were subcutaneously implanted with MDA PCa 173-2 (AR positive, treatment naive adenocarcinoma derived from a primary PCa tumor displaying the T41A mutation),183-A (AR positive, treatment naive adenocarcinoma derived from a PCa bone metastasis), or 180-30 (CRPC primary adenocarcinoma) [16, 21]. When tumors reached 500 mm^3, a subgroup underwent surgical castration. Tumors from intact mice were harvested when they reached 1500 mm [3] (Control). A subgroup of castrated mice was harvested 14 d after castration (early response to castration [ERC]). Remaining mice were monitored over time and considered to have relapsed after 2 weeks of continuous tumor growth (Relapse) after the initial response to the castration [22].

PDX-derived organoids (PDXDO)

Organoids were developed from fresh PDXs as previously described [16]. Briefly, the tissue was chopped, collagenase-II digested, passed through strainers (70/100 μm), centrifuged, and incubated with ACK buffer. Cells were plated in PCM media [16] (2–4 d) and then placed in growth factor–reduced Matrigel supplemented with PCM media.

Drug testing

Organoids were treated with enzalutamide (1–200 μM) or vehicle (DMSO) for 72 h. Treatments with IQ-1 and ICG-001 at different concentrations (2, 5, and 10 μM) were done to block β-catenin/p300 or β-catenin/CBP interactions, respectively. Cell viability was evaluated with CellTiter-Glo® 3D Cell Viability Assay (Promega, Madison, WI).

TCF reporter

β-catenin–mediated transcription was evaluated by reporter assay, using a TOP-flash reporter construct containing 4 consensus TCF-binding sites [23]. Cells were transfected with Lipofectamine 3000 (Invitrogen; Waltham, MA). Reporter activity was assessed at 24 h by a luciferase reporter system (Promega) and normalized to total protein content.

Genetically modified PDX/PDXDO

PDX-derived cells were plated in 24-well plates and transduced with lentiviral particles (OriGene) to express dominant-negative TCF (dnTCF) or empty vector (EV) (plasmids #24311 and #12252; Addgene, Watertown, MA), following manufacturer's protocol (multiplicity of infection: 20). Cells were then processed for organoid formation as described above, under antibiotic selection. Organoids were implanted in mice for propagation.

RNA extraction/RT-qPCR

RNA extraction and complementary DNA (cDNA) preparation were done as reported elsewhere [24]. For PDX samples, RNA was extracted from fresh frozen tissue at the Biospecimen Extraction Facility (MD Anderson). RNA was extracted using Trizol® (Invitrogen) with RNeasy mini kit (QIAGEN; Hilden, Germany), followed by TaqMan reverse transcription reagents (Applied Biosystems), according to the manufacturer's instructions. Real-time (RT)-PCR with SYBR Green dye (Applied Biosystems) and human gene-specific primers were used for cDNA amplification in a QuantStudio3 RT-PCR System (Thermo Fisher Scientific; Waltham, MA). Primer sequences were as follows: *AXIN2*.**F**_5′AGGCCAGTGAGTTGGTTGTC3′/*AXIN2*.**R**_5′ATCTCCTCAAACACCGCTCC3′; *RNF43*.**F**_5′CAAGCTGGAGAGTCCTCGAC3′/*RNF43*.**R**_5′CCATCAGCTTCTCAGCGTCA3′; *ZNRF3*.**F**_5′AGCCAGAATTGGACCCGAAA3′/*ZNRF3*.**R**_5′ACCCTTCACATACACCACCG3′; *NKD1*.**F**_5′ACGTGTTGAGAGACACGCTC3′/*NKD1*.**R**_5′CAGCCCGTCAGTCTTCTCAG3′. Data were normalized to *PPIA* [25] and analyzed using the 2-ΔΔCT method [26].

Immunohistochemistry (IHC) and immunofluorescence (IF)

Formalin-fixed and paraffin-embedded PDX sections were processed, antigen retrieved (citrate) and incubated with anti-β-catenin antibody (1:100; Cell Signaling Technology, Danvers, MA; [#8480]). For IHC, samples were stained with an anti-rabbit IgG (1:500; Invitrogen; #31820) and peroxidase substrate (NovaRED®, Vector Laboratories; Newark, CA) and counterstained with hematoxylin QS (Vector Laboratories). For IF, Alexa 594 anti-rabbit IgG (1:1000; Invitrogen; #A-11012) and 4′,6-diamidino-2-phenylindole (DAPI) were used for staining and counterstaining, respectively.

Datasets

We used the following publicly available datasets.

- Stand-Up to Cancer (SU2C)/Prostate Cancer Foundation and Prostate Cancer Dream Team Consortium [27]. It contains whole-exome sequencing data of 444 CRPC/normal paired samples (429 patients), and gene expression data, measured by RNA-seq, from 266 (polyA)/208 (capture) samples. It includes the Gleason score (GS) at the time of prostatectomy, age, and PSA level at the time of the biopsy. Overall survival (OS) data are available for 128 patients. The dataset was downloaded from cBioPortal using the code "prad_su2c_2019".
- Prostate Adenocarcinoma Project of The Cancer Genome Atlas (TCGA-PRAD) [28]. It contains gene expression information, measured by RNA-seq using Illumina HiSeq (Illumina Inc., California, USA), from 548 samples (497 from primary PCa and 51 samples from adjacent normal tissue) from patients who underwent radical prostatectomy. The dataset includes information on age, PSA levels, GS, tumor stage, exposure to molecular therapy, and radiation therapy. Available time-to-event data includes the progression-free interval for 497 cases and the disease-free interval for 337 cases.
- MDA PCa PDX series (MD Anderson) [16]. Whole-genome, targeted, and RNA-sequencing in representative samples from 44 PDXs derived from 38 patients with clinically annotated, potentially lethal, hormone-naïve PCa or CRPC from primary or different metastatic sites. Data is publicly available in cBioportal https://www.cbioportal.org/study/summary?id=prad_msk_mdanderson_2023) and dbGaP (https://www.ncbi.nlm.nih.gov/gap/), accession number phs003420.v1.p1. MDA PCa PDXs are available through a material transfer agreement. Contact e-mail: pcapdxprogram@mdanderson.org. From this cohort, MDA PCa 280-9, 342-B, and 355-9 models were excluded from analysis based on the following observations from the cohort characterization [16], which interfere with a comprehensive comparison within the cohort: (1) Relativeness analysis indicates that 280-9 and the pair 342-B/355-9 have unique transcriptomic profiles, isolated from the cohort. (2) MDA PCa 342-B and 355-9 are both derived from the same patient at different time points and share a Wnt mutation. Since they are the only sarcomatoid models in the cohort, the lack of "control" models within the morphology/lineage makes them useless for the purpose of this work.
- Paired biopsies from 21 men with metastatic CRPC who underwent tissue biopsy prior to starting enzalutamide treatment and at the time of progression [29].

Bioinformatic analyses

The cBioportal [30] web tool was used to generate OncoPrint plots and differential gene expression analysis. STRING [31] (version 12.0) was used to study interactions

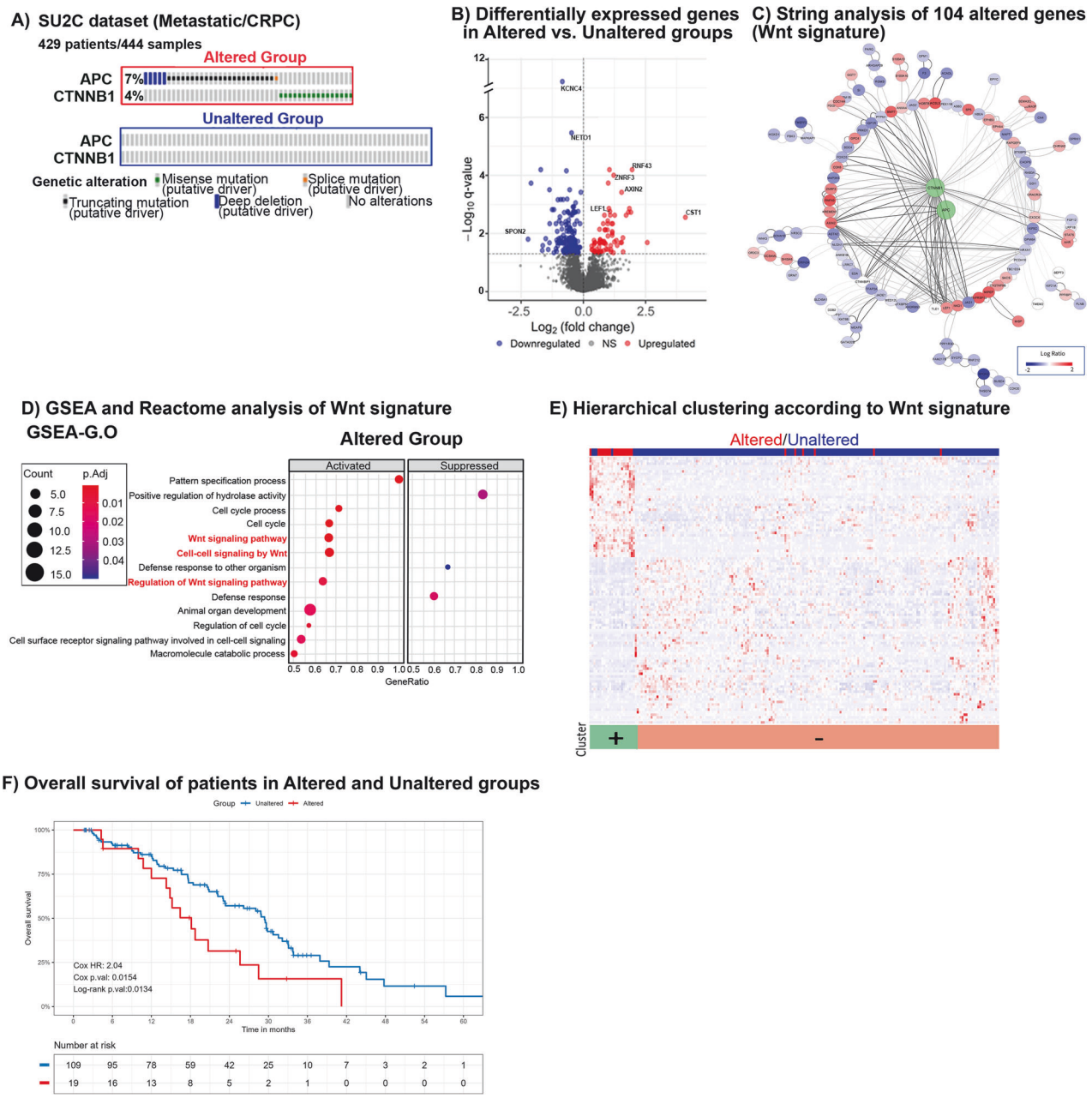

Fig. 1 SU2C database bioinformatics analysis. A Schematic representation of the criteria to group patients with ("Altered Group," red rectangle) or without ("Unaltered Group," blue rectangle) Wnt-activating genomic alterations. **B** Volcano plot of differentially expressed genes in samples with (altered group) or without (unaltered group) Wnt-activating mutations of *CTNNB1* or *APC* from the SU2C dataset. Colored dots are those with significant adjusted *P* values (*Q* values). NS: not significant. **C** Network of 104 genes associated with *CTNNB1* and *APC*, obtained by STRING analysis of differentially expressed genes. **D** Gene set enrichment analysis (GSEA) showing the main Gene Ontology (GO) terms represented by the 104 differentially expressed genes. **E** Unsupervised clustering of SU2C samples based on the expression (heat map) of 104 genes differentially expressed among altered and unaltered groups. **F** Overall survival for patients with (red) or without (blue) alterations in *APC/CTNNB1*.

between proteins (last access: September 2024). Data processing, exploratory analysis, statistical analysis, visualization, and modeling were conducted using the R programming language [32] through RStudio [33].

Survival analysis

Kaplan–Meier curves, log-rank tests, and Cox proportional hazards models were employed for time-to-event analysis using the survminer package in R.

Gene set enrichment analysis (GSEA)

The Wnt-associated genes identified from the SU2C dataset were subjected to GSEA (Broad Institute) (10,000 permutations were run), using the clusterProfiler [34] and enrichplot [35] R packages, the KEGG pathway collection [36], and the Gene Ontology (GO) database [37].

Logistic regressions

Multivariable logistic regression models were constructed using R to investigate the relationship between a binary outcome variable ("presence of activating Wnt mutation" or "Wnt transcriptomic cluster") and multiple predictor variables (previously selected gene set expression levels and AR score). The glm() function (stats package) was employed for model fitting [32]. For each dataset, a separate logistic regression model was fitted.

Receiver operating characteristic (ROC) curves

ROC curves were generated to evaluate the discriminative ability of gene signatures or logistic regression models. The area under the ROC curve (AUC) was calculated as a summary measure of model performance. To statistically compare the performance of the models, DeLong's test for two correlated ROC curves was employed. This non-parametric test assesses whether there is a significant difference between the AUCs of two models. The pROC package [38] in R was used to perform DeLong's test [39] and obtain the corresponding *P* value.

R packages/functions

The tidyverse package [40] was used for general data analysis and manipulation, and the ggplot2 [41], ggpubr [42], and RColorBrewer [43] packages were used to create graphics.

RESULTS

Wnt-driven transcriptomic landscape in advanced PCa

Although the canonical Wnt pathway has been widely studied, the specific targets and mechanisms triggered by uncontrolled Wnt/β-catenin activation in PCa are poorly characterized. Using the SU2C dataset (mCRPC) [27] we explored the differentially expressed genes between samples with or without Wnt-activating alterations in *APC* (7% of patients) or *CTNNB1* (4% of patients) (Fig. 1A) founding 221 significantly deregulated genes (Fig. 1B). Of those, 104 interact with APC and β-catenin in a protein-protein interaction analysis (Fig. 1C) and associated with active Wnt regulation by GSEA (Fig. 1D), consistently grouping APC/CTNNB1 mutated samples in an unsupervised clustering (Fig. 1E). In line with clinical observations [4], patients in SU2C dataset harboring Wnt alterations exhibited impaired OS (Fig. 1F). Thus, these results delineate a clinically relevant Wnt canonical signature in advanced PCa.

MDA PCa PDX models reveal functional Wnt pathway activation

To explore the clinical and biological relevance of these genes, we used previously molecularly characterized models from the MDA PCa PDX series [16]. We determined their Wnt pathway status by

A) Principal component analysis for MDA PCa PDX series according to Wnt signature

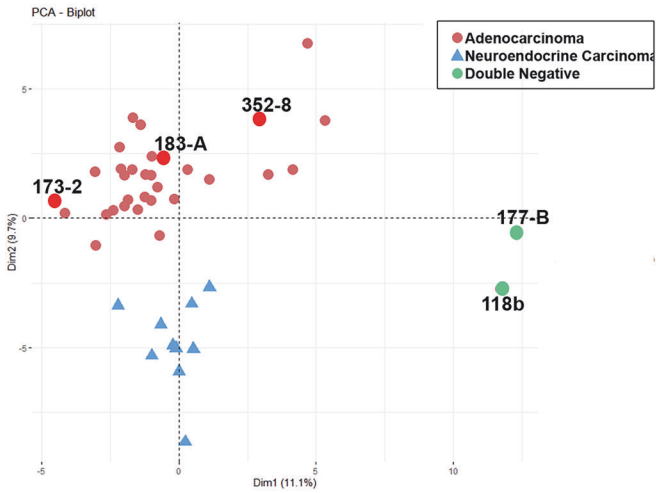

B) Clinical, morphological, and mollecular characteristics of specific PDX models

	MDA PCa PDX				
	183-A	173-2	118b	352-8	177-B
β-catenin IHC	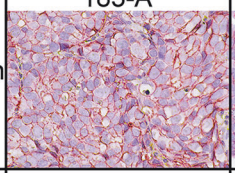	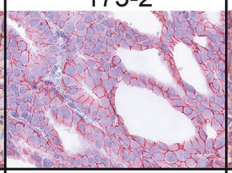	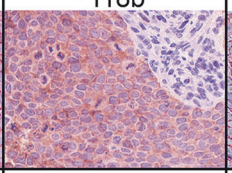	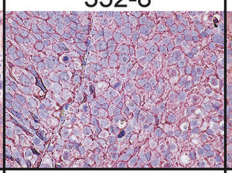	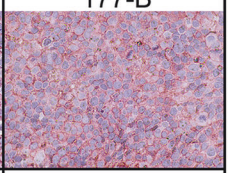
Morph.	Adenocarcinoma	Adenocarcinoma	Adenocarcinoma Double Negative	Adenocarcinoma	Adenocarcinoma Poorly Diff. Double Negative
Wnt activating mutation	———	CTNNB1 T41A (Driver) vaf:0.48	CTNNB1 D32G (Driver) vaf:0.66	APC L1564x (Driver) vaf:0.99	APC S1327*fsd(Driver) vaf:0.98
AR	+	+	-	+	-
Hormone Therapy Status	Naïve	Naïve	CRPC	CRPC	CRPC

Fig. 2 Wnt canonical status in MDA PCa PDX series. A Principal component analysis of the MDA PCa PDX cohort based on Wnt-related genes obtained from the SU2C dataset analysis. **B** Details of β-catenin IHC, morphology, *APC* or *CTNNB1* alterations, AR status, and tumor-of-origin hormone therapy status for MDA PCa 183-A, 173-2, 118b, 352-8, and 177-B.

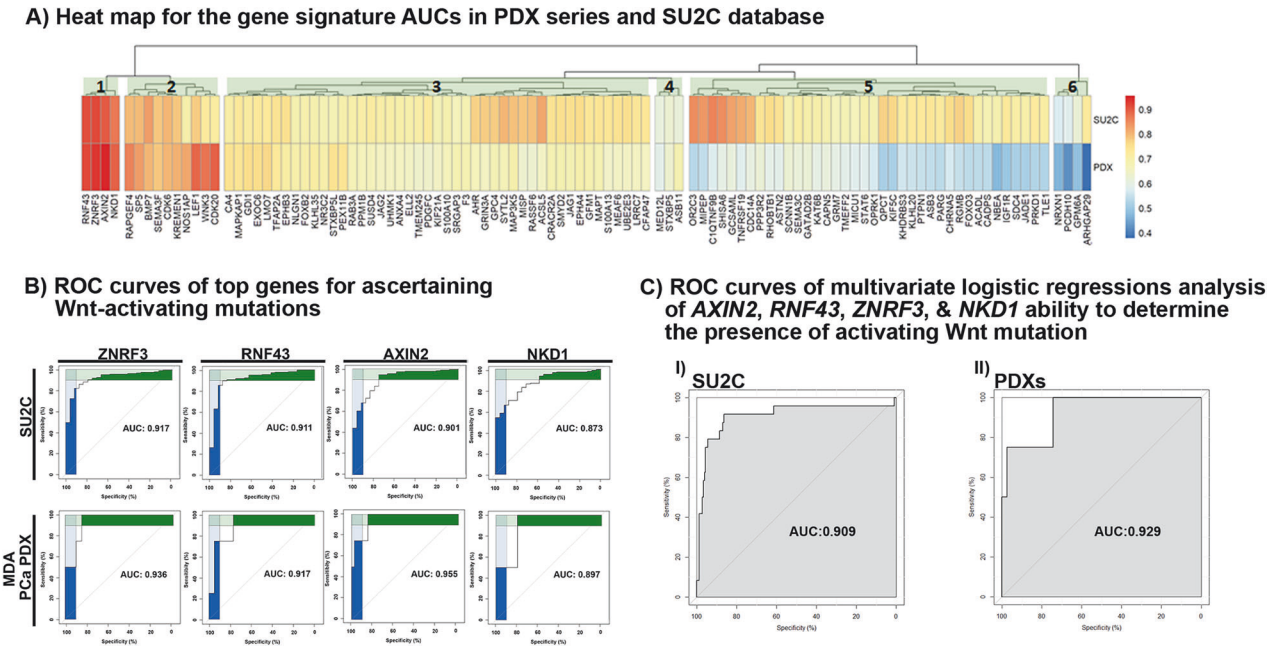

Fig. 3 AXIN2, RNF43, ZNRF3 and NKD1 reflect Wnt canonical status in PCa. A Heatmap for the 104 Wnt-associated genes obtained from SU2C, based on the area under the curve (AUC) of the ROC curve, testing the capacity of these genes to predict the presence of Wnt-activating mutations of *APC* or *CTNNB1* in the SU2C and PDX datasets. Unsupervised clustering was used to group the genes based on their AUC value. **B** ROC curve for the genes with the highest AUC in both SU2C and PDX datasets (*ZNRF3*, *RNF43*, *AXIN2*, *NKD1*). **C** ROC curve for the multivariable logistic regression integrating *AXIN2*, *RNF43*, *ZNRF3*, and *NKD1* for the **I**. SU2C and **II**. PDX datasets.

evaluating the presence of Wnt-activating mutations, β-catenin cellular distribution by IHC, and expression of the 104 Wnt canonical–associated genes identified in human samples (Fig. 1). Interestingly, principal component analysis based on expression of the Wnt-associated genes accurately grouped PDX according to histopathological classification (adenocarcinoma [Adeno], neuroendocrine carcinoma [NE], and double negative models -negative for both, AR and NE markers-[DN]) (Fig. 2A), resulting in segregation of MDA PCa 118b and 177-B, which both harbor known Wnt-activating mutations and cytoplasmic/nuclear β-catenin immunostaining (Fig. 2B). These models grouped within the NE cluster when the same analysis was performed using random genes (Fig. S1), highlighting the capacity of Wnt-associated genes to detect active Wnt pathway in these PDXs models. Despite harboring Wnt-activating mutations, MDA PCa 173-2 and 352-8 clustered with models lacking Wnt alterations (e.g., 183-A) (Fig. 2A), consistent with their β-catenin localization at the plasma membrane. (Fig. 2B). Altogether, these results indicate that the proposed genes accurately distinguish PCa tumors with pathologic Wnt/β-catenin signaling, highlighting the importance of functionally identifying Wnt activity beyond the presence of mutations.

AXIN2, *RNF43*, *ZNRF3*, and *NKD1* reflect Wnt/β-catenin status in PCa

To further tune the transcriptional signature of Wnt activation in PCa, we performed ROC curves associated with the presence of *APC* or *CTNNB1* mutations for each Wnt-associated gene (Fig. 3A). Notably, *ZNRF3*, *RNF43*, *AXIN2*, and *NKD1* (modulators of β-catenin activity) [44–46] emerged as the most robust predictors, consistently achieving the highest AUCs in both the SU2C and PDX datasets (Fig. 3A, B). The combined predictive capacity of these genes using multivariable logistic regression (Fig. S2) achieved AUC values of 0.909 and 0.929 for the SU2C (Fig. 3C.I) and PDX (Fig. 3C.II) datasets, respectively. These results underscore the accuracy of *ZNRF3*, *RNF43*, *AXIN2*, and *NKD1* as reliable indicators of Wnt activation status.

The role of Wnt/β-catenin in regulating these genes was verified by inhibiting β-catenin transcriptional activity using a dnTCF variant (missing the β-catenin binding domain) (Figs. 4A.I and S4) [27]. We genetically engineered MDA PCa 118b-derived organoids to express dnTCF or EV as a control. Organoids were then reimplanted into mice to establish modified PDXs (Fig. 4A.II). Immunofluorescence revealed reduced β-catenin nuclear immunostaining in dnTCF models compared with the EV group, indicating impairment of β-catenin activity (Fig. 4A.III). Consistently, dnTCF expression significantly reduced *AXIN2*, *RNF43*, *ZNRF3*, *and NKD1* expression (Fig. 4B).

AR suppression activates Wnt signaling in mutant β-catenin prostate cancer

Cross-regulation between AR and Wnt/β-catenin pathways has been proposed by others [12–14] and us [24]; however, results are controversial, highlighting the complexity of this interaction [12].

Interestingly, among the four PDX models harboring Wnt driver mutations (118b, 173-2, 177-B, 352-8), only the AR-negative models (118b, 177-B) showed active Wnt signaling (Fig. 2B), in line with a recent report indicating that androgen deprivation therapy (ADT) elevates Wnt/β-catenin signaling activation in DN PCa cells [47], and suggesting that AR can influence Wnt signaling even in the presence of Wnt-activating mutations. Consistent with that, OS and samples clustering based on Wnt-associated genes expression did not show correlation with APC/CTNNB1 alterations in the TCGA-PRAD dataset (primary non-metastatic treatment-naïve PCa) [28] (Fig. S3B, C) despite having a similar alteration frequency as SU2C (Figs. 1A and S3A), suggesting a null/slight impact of these alterations in early disease despite the presence of mutations.

Thus, we investigated how AR inhibition affects mutant β-catenin activity. Enzalutamide treatment (30 μM, 24 h) increased β-catenin activity only when expressing mutant β-catenin variants, as measured by TCF reporter assays in C42B and LNCaP cells (Fig. 5A.I-II); accompanied by the induction of Wnt signature (Fig. 5A.III-IV). These findings indicate that AR inhibition can

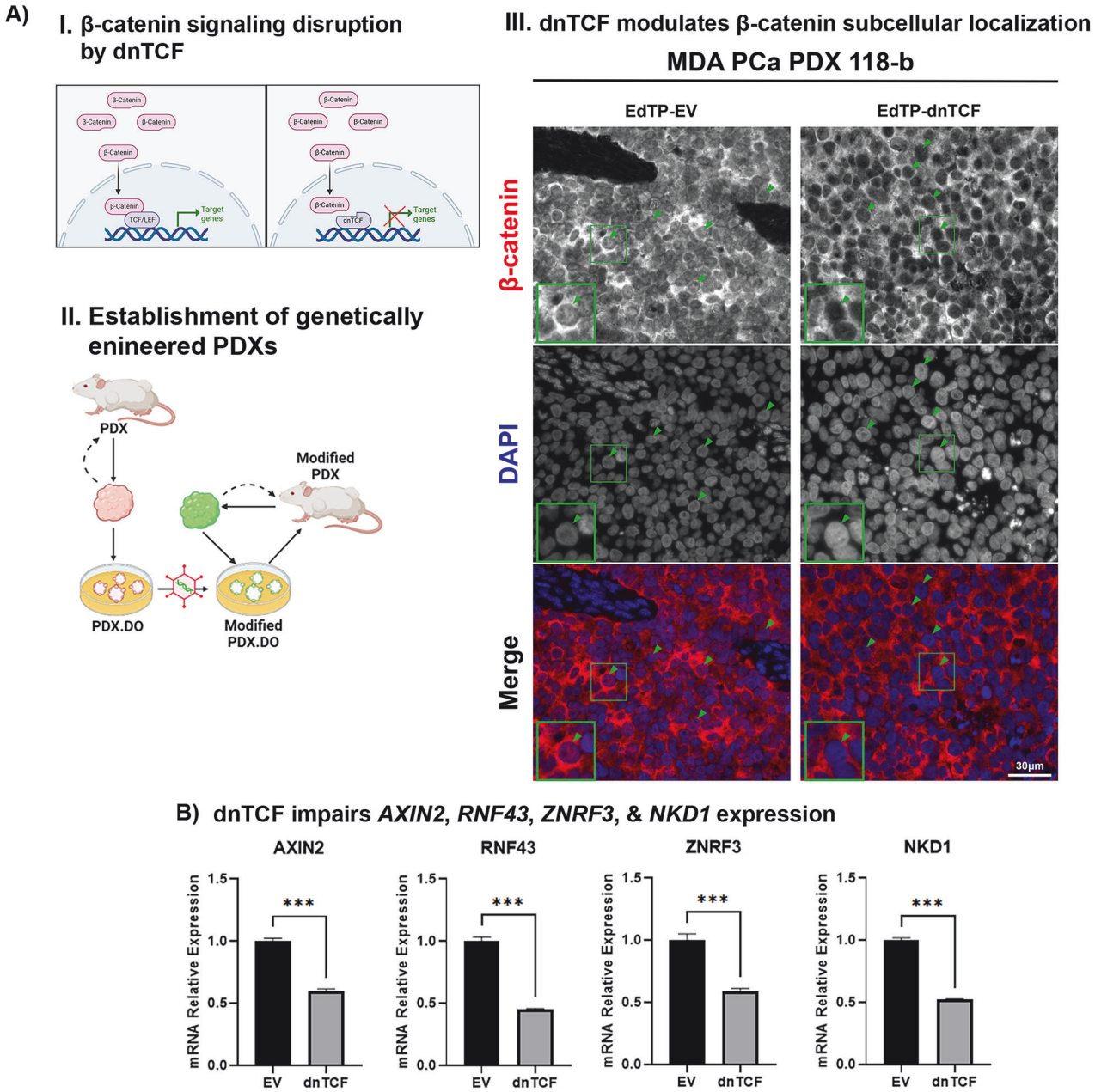

Fig. 4 Functional validation of β-catenin implication on signature modulation. A I. Schematic representation of the effect of dominant-negative TCF (dnTCF) variant on β-catenin signaling. **II**. Schematic representation of the procedure for the establishment of genetically engineered PDX models. Briefly, PDXs were processed, cultured in vitro as PDX-derived organoids (PDXDO), and transduced with lentivirus. Modified organoids underwent selection with antibiotics in vitro and were reimplanted in mice. During 3 passages, modified PDXs underwent antibiotic selection in vitro and then were reimplanted in mice. **III**. Immunofluorescence staining for β-catenin in MDA PCa 118b expressing either empty vector (EV) or dnTCF. In merged images, β-catenin is shown in red and the nucleus (DAPI) in blue. Green arrows indicate the nuclei of specific cells in the images. The squares at the bottom left of each panel show a magnified view of the boxed area. **B** Expression of *AXIN2*, *RNF43*, *ZNRF3*, and *NKD1* (top Wnt-associated genes) evaluated by RT-qPCR in 118b-EV and 118b-dnTCF. Statistical significance assessed by *t* test. Statistical significance: *** $P < 0.001$.

enhance β-catenin activity in PCa models with mutant β-catenin, thereby amplifying Wnt pathway signaling.

Since Wnt-activating mutations have been associated with resistance to AR-targeting treatments [3, 4], we evaluated the in vitro effect of AR inhibition with enzalutamide on the viability of organoids derived from 173-2 (AR^+; $\beta\text{-catenin}^{mut}$) and 183-A ($AR^+$; $\beta\text{-catenin}^{WT}$) (Figs. 5B and S5A). Of note, among the genomic alterations of known PCa-associated genes, both models have PTEN deletion and *TMPRSS2-ERG* fusion, only differing in *CTNNB1* (β-catenin) status [16]. Consistent with our hypothesis, organoids derived from 173-2 exhibited null sensitivity, while 183-A responded to drug treatment in a dose-dependent manner (Fig. 5B.II). To assess response to impaired AR activity in vivo, we surgically castrated mice bearing MDA PCa 173-2 or 183-A growing subcutaneously (Fig. 5C.I). Following an initial response (ERC), only 50% of 183-A tumors relapsed upon castration (Fig. S5B.I), while 86% of 173-2 tumors progressed (Fig. 5C.II) as AR-indifferent PCa (Fig. 5D), consistent with PDXDO results in vitro and resembling an AR^-/CRPC model (Fig. S5B.II). Consistently, expression of Wnt signature genes was significantly induced in

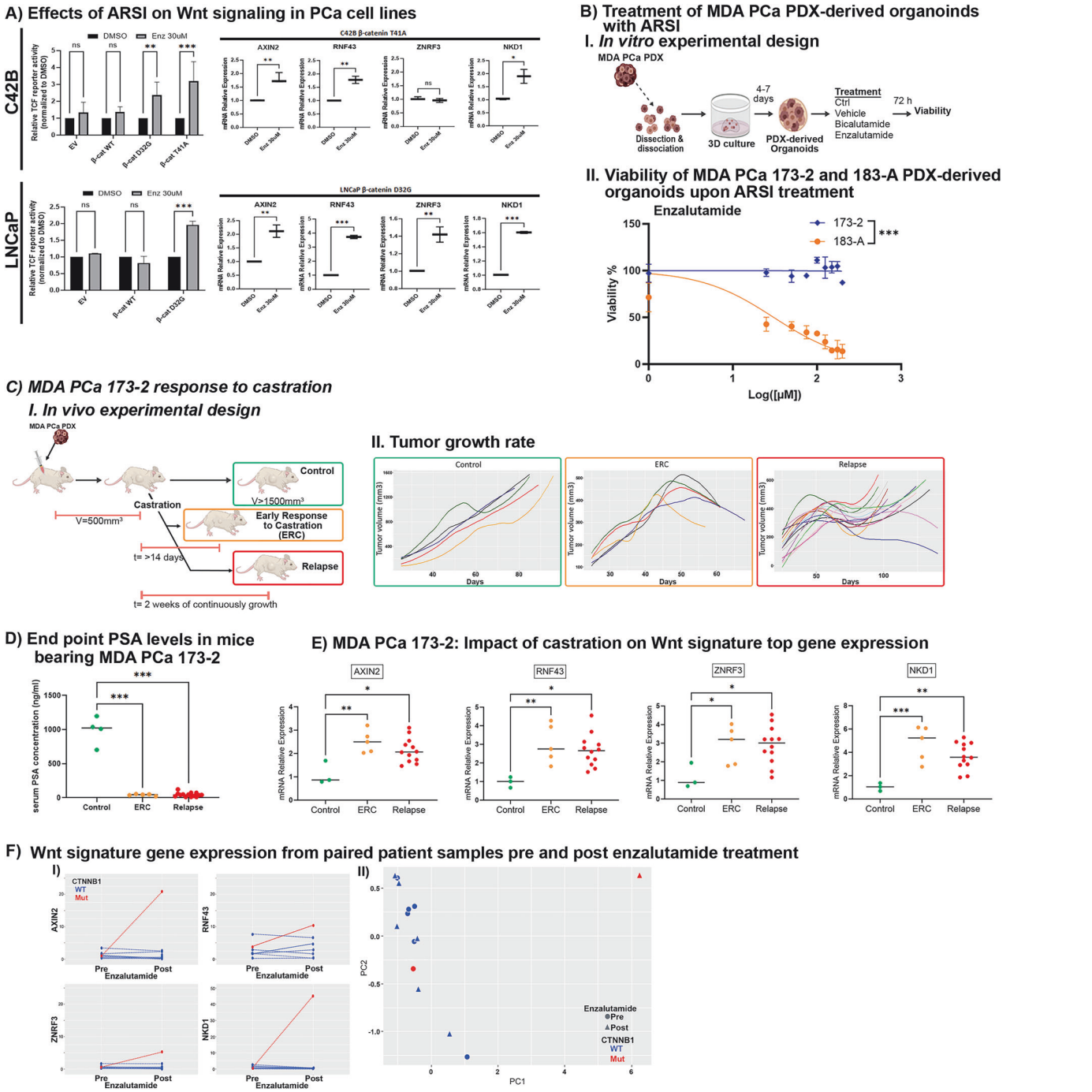

Fig. 5 Crosstalk between AR inhibition and β-catenin activaiton. A TCF reporter activity (left panels) and expression of *AXIN2*, *RNF43*, *ZNRF3*, and *NKD1* evaluated by RT-qPCR (right panels) on C42B and LNCaP cells expressing or not β-catenin WT or mutant variants D32G or T41A under DMSO (vehicle) or enzalutamide treatment (30 μM, 24 H). Statistical significance for TCF reporter activity was assessed by two-way ANOVA and Šídák's multiple comparisons test. Statistical significance for gene expression analysis was assessed by *t* test. **B I**. Schematic representation of PDX-derived organoid drug testing experimental design. **II**. CellTiter-Glo® 3D Cell Viability Assay of organoids derived from MDA PCa 173-2 or 183-A treated with enzalutamide (0–200 μM; 72 H; DMSO as vehicle). Statistical significance assessed by non-linear regression comparison. **C I**. Schematic representation of in vivo castration experimental design. **II**. MDA PCa 173-2 tumor volume curves over time for each mouse in each experimental group. **D** Serum PSA levels measured at endpoint, from mice in each group on castration experiment. **E** Expression of *AXIN2*, *RNF43*, *ZNRF3*, and *NKD1* evaluated by RT-qPCR on 173-2 tumors from each experimental group. Statistical significance assessed by one-way ANOVA. **F** Evaluation of the Wnt signature genes on paired patient samples pre and post enzalutamide treatment. **I**. *AXIN2*, *RNF43*, *ZNRF3*, and *NKD1* expression before and after treatment. **II**. Principal component analysis based on *AXIN2*, *RNF43*, *ZNRF3*, and *NKD1* expression levels. Cases harboring a *CTNNB1* driver mutation are depicted in red. WT: wild type; Mut: mutant. Statistical significance: * $P < 0.05$; ** $P < 0.01$; *** $P < 0.001$.

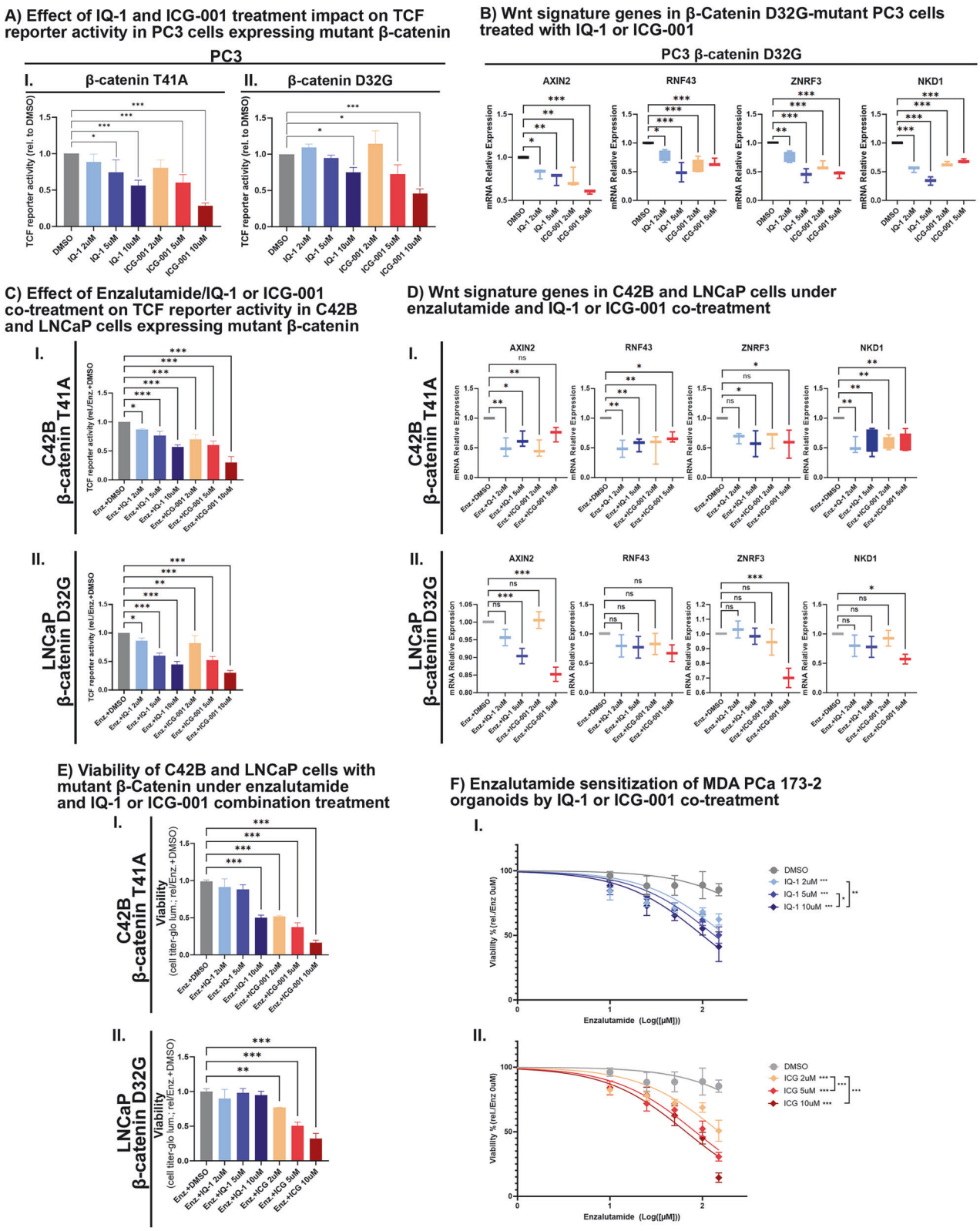

tumors growing in castrated mice (ERC and Relapse) compared with Control (Fig. 5E), indicating activation of the Wnt pathway upon castration and relocating it as a potential driver of progression in an AR-independent scenario.

Consistent with our experimental results, by analyzing longitudinal samples pre/post enzalutamide treatment [29], *AXIN2*, *RNF43*, *ZNRF3*, and *NKD1* increased expression following enzalutamide treatment was observed in apatient with a lymph node (LN) metastasis harboring a *CTNNB1* mutation, while no changes were observed in other LN/LN longitudinal pairs without *CTNNB1* alterations (Fig. 5F.I). Furthermore, the post-treatment mutated sample was distinctly segregated from the others in a principal

Fig. 6 β-catenin co-factors as actionable targets against resistance. A TCF reporter activity on PC3 cells expressing β-catenin mutant variants **I**. T41A or **II**. D32G under IQ-1 or ICG-001 treatment (2, 5 or 10 μM, 24 H. DMSO as vehicle). **B** *AXIN2*, *RNF43*, *ZNRF3*, and *NKD1* (top Wnt signature genes) expression evaluated by RT-qPCR in PC3 cells expressing β-catenin D32G mutant variant treated with IQ-1 or ICG-001 (2 or 5 μM, 24 H. DMSO as vehicle). **C** TCF reporter activity from **I**. C42B and **II**. LNCaP cells expressing β-catenin T41A and D32G mutant variants, respectively, under enzalutamide treatment (30 μM, 24 H) combined or not combined with IQ-1 or ICG-001 (2, 5, or 10 μM, 24 H. DMSO as vehicle). **D** Expression of *AXIN2*, *RNF43*, *ZNRF3*, and *NKD1* (top Wnt signature genes) evaluated by RT-qPCR in **I**. C42B and **II**. LNCaP cells expressing β-catenin T41A and D32G mutant variants, respectively, treated with enzalutamide (30 μM, 24 H) combined or not combined with IQ-1 or ICG-001 (2, 5, or 10 μM, 24 H. DMSO as vehicle). **E** CellTiter-Glo® Cell Viability Assay of **I**. C42B and **II**. LNCaP cells expressing β-catenin T41A and D32G mutant variants, respectively, under enzalutamide treatment (30 μM, 24 H) combined or not combined with IQ-1 or ICG-001 (2, 5, or 10 μM, 72 H). DMSO as vehicle). **F** CellTiter-Glo® 3D Cell Viability Assay of organoids derived from MDA PCa 173-2 treated with enzalutamide (0–150 μM), combined or not combined with **I**. IQ-1 or **II**. ICG-001 (2, 5, or 10 μM) (72 H; DMSO as vehicle). Statistical significance was assessed by one-way ANOVA or non-linear regression comparison. Statistical significance: * $P < 0.05$; ** $P < 0.01$; *** $P < 0.001$.

component analysis based on the expression of this signature (Fig. 5F.II), highlighting the clinical impact of ARSI treatment on Wnt pathway activity in PCa with mutant β-catenin.

Together, these results show that PDX/PDXDO models recapitulate clinical observations, highlighting the critical role of Wnt signaling in ARSI treatment outcomes. This suggests that mutation-driven Wnt activation can be triggered upon AR inhibition, underscoring the need to consider this pathway in therapeutic strategies.

Targeting β-Catenin/co-factors interaction to overcome Wnt-driven resistance in PCa

Different programs can be triggered downstream of β-catenin activation depending on its interaction with different co-activators, including p300 and CREB-binding protein (CBP) [42, 43]. These factors can also interact with nuclear receptors, including AR [48]. Thus, p300 and CBP emerge not only as potential mediators of β-catenin/AR cross-regulation but also as attractive targets for halting Wnt-driven progression. We tested two different compounds, IQ-1 (β-catenin/p300 interaction blocker) and ICG-001 (β-catenin/CBP interaction blocker), at different concentrations (2, 5, and 10 μM). Both compounds significantly downregulated TCF reporter activity in PC3 cells expressing mutant β-catenin variants (Fig. 6A). Consistently, mRNA expression levels of *AXIN2*, *RNF43*, *ZNRF3*, and *NKD1* were significantly suppressed upon treatment with both IQ-1 and ICG-001 in these cells (Fig. 6B). Strikingly, co-treating LNCaP and C42B cells harboring β-catenin active variants with enzalutamide and IQ-1 or ICG-001 significantly repressed the induction of TCF reporter activity (Fig. 6C) and Wnt signature expression (Fig. 6D) caused by single-agent enzalutamide (Fig. 5A). Moreover, combining enzalutamide, either with IQ-1 or ICG-001 exerted a significant reduction in cell viability compared with enzalutamide monotherapy (Fig. 6E). Consistently, either IQ-1 or ICG-001 sensitized MDA PCa PDX 173-2 (harboring endogenous β-catenin activating-mutation) derived organoids to enzalutamide under a co-treatment regimen (Fig. 6F), alongside Wnt signature modulation (Fig. S6). This suggests that impairing β-catenin signaling by targeting its interaction with CBP or p300 can effectively overcome intrinsic resistance to enzalutamide, thereby restoring drug efficacy in PCa models with Wnt alterations. Altogether, these findings suggest that targeting β-catenin signaling by blocking its interaction with p300 or CBP is a promising therapeutic strategy for Wnt-driven tumors and could enhance the anti-tumor efficacy of enzalutamide by preventing Wnt-driven resistance in PCa.

DISCUSSION

PCa is characterized by significant interpatient heterogeneity of treatment response [1, 2]. The Wnt canonical pathway has emerged as a candidate that may support CRPC progression in patients with specific mutations [3, 4], but the implications and underlying mechanisms of Wnt pathway alterations are still being deciphered. This study provides new insights into the role of Wnt canonical pathway activation in PCa progression and its interaction with AR signaling.

In this study, we identified a discrete transcriptional gene signature (*AXIN2*, *RNF43*, *ZNRF3*, and *NKD1*) that accurately reflects mutation-driven Wnt pathway activation in PCa. Of note, Tang and colleagues [49] proposed an epigenomic Wnt signature encompassing *AXIN2*, *RNF43*, *CTNNB1* and *TCF7L2*. However, we did not find an association between *CTNNB1* and *TCF7L2* mRNA levels with mutation-driven-pathway activation.

Moreover, we showcased that mutation-driven Wnt/β-catenin activation is intricately linked to resistance to ARSI, a standard therapeutic approach for advanced disease. We demonstrated that AR suppression amplifies β-catenin activity in tumors harboring Wnt-activating mutations, revealing a clinically relevant crosstalk between both pathways that drives ARSI resistance. The cross-regulation between AR and Wnt/β-catenin has been proposed in previous studies [12–14, 50–56], but results are controversial, reflecting the complexity of this interaction affecting both pathways in a context-dependent manner [12]. Nevertheless, those studies were mainly focused on the impact on AR activity and did not consider Wnt mutations, which are the primary context for pathological Wnt activation in PCa [10, 11, 55]. Our findings strengthen the hypothesis that Wnt signaling drives tumor progression in a subset of patients when AR is suppressed, supporting its role as a crucial player in the development of treatment resistance.

CBP and p300, downstream coactivators of β-catenin signaling, emerged as potential mediators of the β-catenin/AR cross-regulation. These coactivators play nonredundant roles in β-catenin–driven transcription but also interact with nuclear receptors, including AR [48, 57, 58]. Of note, targeting β-catenin/CBP significantly reduced tumor stemness and treatment resistance in cervical cancer and leukemia [59, 60], while CBP and p300 expression levels have been associated with the development of ADT resistance in both primary and metastatic PCa [61].

Our data shows that pharmacologic blockade of β-catenin/CBP or β-catenin/p300 interactions restores sensitivity to ARSI in models harboring Wnt-activating mutations, underscoring their potential therapeutic relevance. The differential response within different PCa models to enzalutamide combined with CBP/p300 inhibition emphasizes how lineage context and intrinsic drug sensitivity shape Wnt-transcriptional output. These findings highlight that therapeutic strategies must account not only for β-catenin variants but also for coactivator availability and ARSI responsiveness when interpreting Wnt pathway activity in PCa.

Altogether, these findings strengthen the hypothesis that Wnt signaling drives tumor progression in a subset of patients when AR is suppressed and support the development of combination strategies targeting AR and Wnt pathways. Such approaches may expand treatment options for patients with ARSI resistance and Wnt-activating mutations.

CONCLUSION

This study uncovers a critical crosstalk between canonical Wnt signaling and ARSI in PCa, mediated by CBP and p300 as nonredundant coactivators of β-catenin/AR cross-regulation. AR

suppression enhances β-catenin activity in tumors with Wnt-activating mutations, driving resistance to AR-targeted therapies. Pharmacologic disruption of β-catenin interactions with CBP or p300 restores ARSI sensitivity in preclinical models, providing a strong rationale for co-targeting AR and Wnt pathways.

DATA AVAILABILITY

The datasets analyzed during the current study are publicly available, as stated in the Methods section. MDA PCa PDXs are available through a material transfer agreement. Contact e-mail: pcapdxprogram@mdanderson.org.

REFERENCES

1. Watson PA, Arora VK, Sawyers CL. Emerging mechanisms of resistance to androgen receptor inhibitors in prostate cancer. Nat Rev Cancer. 2015;15:701–11.
2. Jamroze A, Chatta G, Tang DG. Androgen receptor (AR) heterogeneity in prostate cancer and therapy resistance. Cancer Lett. 2021;518:1–9.
3. Wang L, Dehm SM, Hillman DW, Sicotte H, Tan W, Gormley M, et al. A prospective genome-wide study of prostate cancer metastases reveals association of wnt pathway activation and increased cell cycle proliferation with primary resistance to abiraterone acetate–prednisone. Ann Oncol. 2018;29:352–60.
4. Isaacsson Velho P, Fu W, Wang H, Mirkheshti N, Qazi F, Lima FAS, et al. Wnt-pathway activating mutations are associated with resistance to first-line abiraterone and enzalutamide in castration-resistant prostate cancer. Eur Urol. 2020;77:14–21.
5. Nandana S, Tripathi M, Duan P, Chu CY, Mishra R, Liu C, et al. Bone metastasis of prostate cancer can be therapeutically targeted at the TBX2-WNT signaling axis. Cancer Res. 2017;77:1331–44.
6. Vallée A, Lecarpentier Y, Vallée JN. Curcumin: a therapeutic strategy in cancers by inhibiting the canonical WNT/β-catenin pathway. J Exp Clin Cancer Res. 2019;38:1–16.
7. Lecarpentier Y, Schussler O, Hébert JL, Vallée A. Multiple targets of the canonical WNT/β-catenin signaling in cancers. Front Oncol. 2019;9:1–17.
8. Tarapore RS, Siddiqui IA, Mukhtar H. Modulation of Wnt/ -catenin signaling pathway by bioactive food components. Carcinogenesis. 2012;33:483–91.
9. Houschyar KS, Tapking C, Borrelli MR, Popp D, Duscher D, Maan ZN, et al. Wnt pathway in bone repair and regeneration–what do we know so far? Front Cell Dev Biol. 2019;6:1–13.
10. Chung JH, Dewal N, Sokol E, Mathew P, Whitehead R, Millis SZ, et al. Prospective comprehensive genomic profiling of primary and metastatic prostate tumors. JCO Precis Oncol. 2019;3:1–23.
11. Robinson D, Van Allen EM, Wu YM, Schultz N, Lonigro RJ, Mosquera JM, et al. Integrative clinical genomics of advanced prostate cancer. Cell. 2015;161:1215–28.
12. Schweizer L, Rizzo CA, Spires TE, Platero JS, Wu Q, Lin TA, et al. The androgen receptor can signal through Wnt/β-Catenin in prostate cancer cells as an adaptation mechanism to castration levels of androgens. BMC Cell Biol. 2008;9:1–15.
13. Lee E, Ha S, Logan SK. Divergent androgen receptor and beta-catenin signaling in prostate cancer cells. PLoS ONE. 2015;10:e0141589.
14. Kretzschmar K, Cottle DL, Schweiger PJ, Watt FM. The androgen receptor antagonizes Wnt/β-catenin signaling in epidermal stem cells. J Investig Dermatol. 2015;135:2753–63.
15. Robinson D, Van Allen EM, Wu Y-M, Schultz N, Lonigro RJ, Mosquera J-M, et al. Integrative clinical genomics of advanced prostate cancer. Cell. 2015;161:1215–28.
16. Anselmino N, Labanca E, Shepherd PDA, Dong J, Yang J, Song X, et al. Integrative molecular analyses of the MD Anderson prostate cancer patient-derived xenograft (MDA PCa PDX) series. Clin Cancer Res. 2024;30:2272–85.
17. OncoKB. https://www.oncokb.org/
18. COSMIC. https://cancer.sanger.ac.uk/cosmic
19. Cancer Hotspots. https://www.cancerhotspots.org/.
20. Kim S, Jeong S. Mutation hotspots in the β-catenin gene: lessons from the human cancer genome databases. Mol Cells. 2019;42:8–16.
21. Palanisamy N, Yang J, Shepherd PDA, Li-Ning-Tapia EM, Labanca E, Manyam GC, et al. The MD Anderson prostate cancer patient-derived xenograft series (MDA PCa PDX) captures the molecular landscape of prostate cancer and facilitates marker-driven therapy development. Clin Cancer Res. 2020;26:4933–46.
22. Labanca E, Bizzotto J, Sanchis P, Anselmino N, Yang J, Shepherd PDA, et al. Prostate cancer castrate resistant progression usage of non-canonical androgen receptor signaling and ketone body fuel. Oncogene. 2021;40:6284–98.
23. Korinek V, Barker N, Morin PJ, van Wichen D, de Weger R, Kinzler KW, et al. Constitutive transcriptional activation by a β-catenin-Tcf complex in APC $^{-/-}$ colon carcinoma. Science. 1997;275:1784–7.
24. Wan X, Liu J, Lu JF, Tzelepi V, Yang J, Starbuck MW, et al. Activation of β-catenin signaling in androgen receptor-negative prostate cancer cells. Clin Cancer Res. 2012;18:726–36.
25. Vajda A, Marignol L, Barrett C, Madden SF, Lynch TH, Hollywood D, et al. Gene expression analysis in prostate cancer: the importance of the endogenous control. Prostate. 2013;73:382–90.
26. Livak KJ, Schmittgen TD. Analysis of relative gene expression data using real-time quantitative PCR and the $2^{-\Delta\Delta CT}$ method. Methods. 2001;25:402–8.
27. Abida W, Cyrta J, Heller G, Prandi D, Armenia J, Coleman I, et al. Genomic correlates of clinical outcome in advanced prostate cancer. Proc Natl Acad Sci USA. 2019;116:11428–36.
28. The Cancer Genome Atlas. TCGA. http://cancergenome.nih.gov/.
29. Westbrook TC, Guan X, Rodansky E, Flores D, Liu CJ, Udager AM, et al. Transcriptional profiling of matched patient biopsies clarifies molecular determinants of enzalutamide-induced lineage plasticity. Nat Commun. 2022;13:5345.
30. Cerami E, Gao J, Dogrusoz U, Gross BE, Sumer SO, Aksoy BA, et al. The cBio cancer genomics portal: an open platform for exploring multidimensional cancer genomics data. Cancer Discov. 2012;2:401–4.
31. Szklarczyk D, Gable AL, Nastou KC, Lyon D, Kirsch R, Pyysalo S, et al. The STRING database in 2021: customizable protein–protein networks, and functional characterization of user-uploaded gene/measurement sets. Nucleic Acids Res. 2021;49:D605–12.
32. R Core Team. R: the R project for statistical computing. https://www.r-project.org/
33. RStudio Team. RStudio: integrated development environment for R. Boston. 2015. http://www.rstudio.com/
34. Wu T, Hu E, Xu S, Chen M, Guo P, Dai Z, et al. clusterProfiler 4.0: A universal enrichment tool for interpreting omics data. Innovation. 2021;2:100141.
35. Yu G. Enrichplot: visualization of functional enrichment result. https://doi.org/10.18129/B9.bioc.enrichplot, R package version 1.22.0, https://bioconductor.org/packages/enrichplot 2023.
36. Kanehisa M, Sato Y, Kawashima M, Furumichi M, Tanabe M. KEGG as a reference resource for gene and protein annotation. Nucleic Acids Res. 2016;44:D457–62.
37. Ashburner M, Ball CA, Blake JA, Botstein D, Butler H, Cherry JM, et al. Gene Ontology: a tool for the unification of biology. Nat Genet. 2000;25:25–29.
38. Robin X, Turck N, Hainard A, Tiberti N, Lisacek F, Sanchez J-C, et al. pROC: an open-source package for R and S+ to analyze and compare ROC curves. BMC Bioinforma. 2011;12:77.
39. DeLong ER, DeLong DM, Clarke-Pearson DL. Comparing the areas under two or more correlated receiver operating characteristic curves: a nonparametric approach. Biometrics. 1988;44:837–45.
40. Wickham H, Averick M, Bryan J, Chang W, McGowan L, François R, et al. Welcome to the tidyverse. J Open Source Softw. 2019;4:1686.
41. Wickham H. ggplot2. Springer International Publishing: Cham; 2016. https://doi.org/10.1007/978-3-319-24277-4.
42. Alboukadel Kassambara. ggpubr: "ggplot2" based publication-ready plots. 2023.https://rpkgs.datanovia.com/ggpubr/.
43. Neuwirth E. RColorBrewer: ColorBrewer Palettes 2022.https://CRAN.R-project.org/package=RColorBrewer.
44. Zhan T, Rindtorff N, Boutros M. Wnt signaling in cancer. Oncogene. 2017;36:1461–73.
45. van Amerongen R, Nusse R. Towards an integrated view of Wnt signaling in development. Development. 2009;136:3205–14.
46. Angonin D, Van Raay TJ. Nkd1 functions as a passive antagonist of Wnt signaling. PLoS ONE. 2013;8:e74666.
47. Kim WK, Buckley AJ, Lee DH, Hiroto A, Nenninger CH, Olson AW, et al. Androgen deprivation induces double-null prostate cancer via aberrant nuclear export and ribosomal biogenesis through HGF and Wnt activation. Nat Commun. 2024;15. https://doi.org/10.1038/s41467-024-45489-4.
48. Ono M, Lai KKY, Wu K, Nguyen C, Lin DP, Murali R, et al. Nuclear receptor/Wnt beta-catenin interactions are regulated via differential CBP/ p300 coactivator usage. PLoS ONE. 2018;13. https://doi.org/10.1371/journal.pone.0200714.
49. Tang F, Xu D, Wang S, Wong CK, Martinez-Fundichely A, Lee CJ, et al. Chromatin profiles classify castration-resistant prostate cancers, suggesting therapeutic targets. Science. 2022;376. https://doi.org/10.1126/science.abe1505.
50. Khurana N, Sikka SC. Interplay between SOX9, Wnt/β-catenin and androgen receptor signaling in castration-resistant prostate cancer. Int J Mol Sci. 2019;20. https://doi.org/10.3390/ijms20092066.
51. Wang G, Wang J, Sadar MD. Crosstalk between the Androgen receptor and β-catenin in castrate-resistant prostate cancer. Cancer Res. 2008;68:9918–27.
52. Wang C, Chen Q, Xu H. Wnt/β-catenin signal transduction pathway in prostate cancer and associated drug resistance. Discov Oncol. 2021;12:2–12.
53. Singh R, Bhasin S, Braga M, Artaza JN, Pervin S, Taylor WE, et al. Regulation of myogenic differentiation by androgens: cross-talk between androgen receptorβ-catenin and follistatin/transforming growth factor-β signaling pathways. Endocrinology. 2009;150:1259–68.

54. Cristóbal I, Rojo F, Madoz-Gúrpide J, García-Foncillas J. Cross talk between Wnt/β-catenin and CIP2A/Plk1 signaling in prostate cancer: promising therapeutic implications. Mol Cell Biol. 2016;36:1734–9.
55. Schneider JA, Logan SK. Revisiting the role of Wnt/β-catenin signaling in prostate cancer. Mol Cell Endocrinol. 2018;462:3–8.
56. Terry S, Yang X, Chen M-W, Vacherot F, Buttyan R. Multifaceted interaction between the androgen and Wnt signaling pathways and the implication for prostate cancer. J Cell Biochem. 2006;99:402–10.
57. Miyabayashi T, Teo J-L, Yamamoto M, McMillan M, Nguyen C, Kahn M. Wnt/β-catenin/CBP signaling maintains long-term murine embryonic stem cell pluripotency. Proc Natl Acad Sci. 2007;104:5668–73.
58. Ma H, Nguyen C, Lee KS, Kahn M. Differential roles for the coactivators CBP and p300 on TCF/β-catenin-mediated survivin gene expression. Oncogene. 2005;24:3619–31.
59. Zhao Y, Masiello D, McMillian M, Nguyen C, Wu Y, Melendez E, et al. CBP/catenin antagonist safely eliminates drug-resistant leukemia-initiating cells. Oncogene. 2016;35:3705–17.
60. Feng D, Yan K, Liang H, Liang J, Wang W, Yu H, et al. CBP-mediated Wnt3a/β-catenin signaling promotes cervical oncogenesis initiated by Piwil2. Neoplasia. 2021;23:1–11.
61. Welti J, Sharp A, Brooks N, Yuan W, McNair C, Chand SN, et al. Targeting the p300/CBP axis in lethal prostate cancer. Cancer Discov. 2021;11:1118–37.

ACKNOWLEDGEMENTS

We would like to express our deepest gratitude to Dr. Nora Navone, whose invaluable guidance and support greatly influenced this work. Her legacy continues to inspire us, and her contributions will always be remembered. We thank Sarah E. Townsend for editing the article. We are grateful to the Office for Postdoctoral Fellows at The University of Texas MD Anderson Cancer Center for supporting Nicolas Anselmino through both an Endowed Fellowship Research Award and the Ben Love Fellowship in Innovative Cancer Therapy Pilot Grant.

AUTHOR CONTRIBUTIONS

Conceptualization and design: NA. Acquisition of data: NA, PS, and JD. Analysis and interpretation of data: NA, PS, JAB. Drafting of the manuscript: NA, PS, and JAB. Critical revision of the manuscript for important intellectual content: NA, PS, JAB, EL, ESV, JM, GG, and CJL. Statistical analysis: NA, PS, and JAB. Obtaining funding: NA, GG, and CJL. Administrative, technical, or material support: EL, JD, PDAS, and JY. Supervision: NA and CJL.

FUNDING

This work was supported by a DOD Award (W81XWH-18-1-0171); the Prostate Cancer Foundation; NCI Cancer Center Support Grant (P30CA16672); Agencia Nacional de Promoción de la Investigación, el Desarrollo Tecnológico y la Innovación (ANPCyT), Argentina (PICT-2021-III-A00080); MD Anderson Cancer Center Prostate Cancer SPORE (NIH/NCI P50 CA140388); David H. Koch Center for Applied Research in Genitourinary Cancers at MD Anderson (Houston, TX), NIH/NCI U01 CA224044, and the Scientific Foundation of the Spanish Association against Cancer (AECC) (TALEN246589ANSE) and the European Union through the AECC Talent Programme (GA101081298).

COMPETING INTERESTS

The authors declare no competing interests.

ETHICS

The study used established human cell lines from qualified repositories. All practices involving animals were approved by the Institutional Animal Care and Use Committee of The University of Texas MD Anderson Cancer Center (MDACC), under the regulation of the Animal Welfare Committee and conform to the NIH Policy on Human Care and Use of Laboratory Animals (protocol: #00001091-RN03). The PDX models used in this study were generated by the MDA PCa PDX Program (pcapdxprogram@mdanderson.org) from prostate cancer tissue obtained during therapeutic or diagnostic procedures, including radical prostatectomies, orthopedic and neurosurgical interventions performed to palliate complications, and biopsies of metastatic lesions. Written informed consent was obtained from patients before sample acquisition, and all samples were processed according to a protocol approved by the Institutional Review Board of the University of Texas MD Anderson Cancer Center.

ADDITIONAL INFORMATION

Supplementary information The online version contains supplementary material available at https://doi.org/10.1038/s41418-026-01732-7.

Correspondence and requests for materials should be addressed to Nicolas Anselmino.